

Uniform wafer-scale MOCVD homoepitaxy of β-Ga_2O_3 on 2-inch (010) substrates

Xuanze Zhou(周选择), Haozhong Wu(吴昊中), Yuanjie Ding(丁元杰), Ziyuan Wang(王子原), Zhiyu Zhou(周智宇), Ning Xia(夏宁), Song Zhang(张嵩), Guangwei Xu(徐光伟), Hui Zhang(张辉), and Shibing Long(龙世兵)
Citation: Chin. Phys. B, 2026, 35 (**1**): 016801. DOI: 10.1088/1674-1056/ae12e0
http://cpb.iphy.ac.cn; http://iopscience.iop.org/cpb

What follows is a list of articles you may be interested in

Effects of Mg-doping temperature on the structural and electrical properties of nonpolar *a*-plane p-type GaN films

Kai Chen(陈凯), Jianguo Zhao(赵见国), Yu Ding(丁宇), Wenxiao Hu(胡文晓), Bin Liu(刘斌), Tao Tao(陶涛), Zhe Zhuang(庄喆), Yu Yan(严羽), Zili Xie(谢自力), Jianhua Chang(常建华), Rong Zhang(张荣), and Youliao Zheng(郑有炓)
Chin. Phys. B, 2024, 33 (**1**): 016801. DOI: 10.1088/1674-1056/acdc0b

Three-dimensional vertical ZnO transistors with suspended top electrodes fabricated by focused ion beam technology

Chi Sun(孙驰), Linyuan Zhao(赵林媛), Tingting Hao(郝婷婷), Renrong Liang(梁仁荣), Haitao Ye(叶海涛), Junjie Li(李俊杰), and Changzhi Gu(顾长志)
Chin. Phys. B, 2022, 31 (**1**): 016801. DOI: 10.1088/1674-1056/ac34fe

Epitaxial growth of antimony nanofilms on HOPG and thermal desorption to control the film thickness

Shuya Xing(邢淑雅), Le Lei(雷乐), Haoyu Dong(董皓宇), Jianfeng Guo(郭剑峰), Feiyue Cao(曹飞跃), Shangzhi Gu(顾尚志), Sabir Hussain, Fei Pang(庞斐), Wei Ji(季威), Rui Xu(许瑞), Zhihai Cheng(程志海)
Chin. Phys. B, 2020, 29 (**9**): 096801. DOI: 10.1088/1674-1056/aba27c

Selective linear etching of monolayer black phosphorus using electron beams

Yuhao Pan(潘宇浩), Bao Lei(雷宝), Jingsi Qiao(乔婧思), Zhixin Hu(胡智鑫), Wu Zhou(周武), Wei Ji(季威)
Chin. Phys. B, 2020, 29 (**8**): 086801. DOI: 10.1088/1674-1056/ab9438

Scalable preparation of water-soluble ink of few-layered WSe_2 nanosheets for large-area electronics

Guoyu Xian(冼国裕), Jianshuo Zhang(张建烁), Li Liu(刘丽), Jun Zhou(周俊), Hongtao Liu(刘洪涛), Lihong Bao(鲍丽宏), Chengmin Shen(申承民), Yongfeng Li(李永峰), Zhihui Qin(秦志辉), Haitao Yang(杨海涛)
Chin. Phys. B, 2020, 29 (**6**): 066802. DOI: 10.1088/1674-1056/ab889e

---

Uniform wafer-scale MOCVD homoepitaxy of β-Ga_2O_3 on 2-inch (010) substrates

Xuanze Zhou(周选择)[1], Haozhong Wu(吴昊中)[1], Yuanjie Ding(丁元杰)[1], Ziyuan Wang(王子原)[1], Zhiyu Zhou(周智宇)[1], Ning Xia(夏宁)[2], Song Zhang(张嵩)[3,4,†], Guangwei Xu(徐光伟)[1,‡], Hui Zhang(张辉)[2], and Shibing Long(龙世兵)[1]

[1] *School of Microelectronics, University of Science and Technology of China, Hefei* 230026, *China*
[2] *Hangzhou Garen Semiconductor Company Limited, Hangzhou* 311200, *China*
[3] *The* 46th *Research Institute, China Electronics Technology Group Corporation, Tianjin* 300220, *China*
[4] *CETC Key Laboratory of Advanced Semiconductor Crystal Materials and Technologies, Tianjin* 300220, *China*

(Received 19 September 2025; revised manuscript received 13 October 2025; accepted manuscript online 14 October 2025)

The (010) orientation of β-Ga_2O_3 is a highly promising platform for next-generation lateral power electronics due to its superior theoretical transport properties. However, progress has been impeded by the unavailability of large-area substrates, limiting studies to small-scale samples. Leveraging the recent emergence of 2-inch wafers, we report the first demonstration of homoepitaxial growth on a 2-inch, Fe-doped semi-insulating (010) β-Ga_2O_3 substrate by metal–organic chemical vapor deposition (MOCVD). A systematic, wafer-scale characterization reveals the successful growth of a high-quality epitaxial film. High-resolution x-ray diffraction shows an excellent crystalline structure, with a rocking curve full-width ranging from 21.0 arcsec to 103.0 arcsec. Atomic force microscopy confirms an atomically smooth surface with a root-mean-square roughness below 1.53 nm, displaying a distinct step-flow growth mode across the wafer. Furthermore, mercury-probe capacitance–voltage mapping indicates a well-controlled carrier concentration of $\sim 2 \times 10^{18}$ cm^{-3} with a RSD of 5.12%. This work provides the first comprehensive assessment of 2-inch (010) Ga_2O_3 epitaxial wafers, validating a critical material platform for the development and future manufacturing of high-performance power devices.

Keywords: β-Ga_2O_3, metal–organic chemical vapor deposition (MOCVD), wafer scale, uniformity

PACS: 68.35.bg, 84.30.Jc, 81.10.Bk, 81.15.Kk

DOI: 10.1088/1674-1056/ae12e0 **CSTR:** 32038.14.CPB.ae12e0

1. Introduction

The relentless pursuit of higher efficiency and power density in electronic systems has driven extensive research into ultrawide bandgap (UWBG) semiconductors. Among them, the monoclinic β-phase of gallium oxide (β-Ga_2O_3) has garnered immense attention as a promising material for next-generation power electronics.[1] Its exceptional intrinsic properties, including a bandgap of approximately 4.8 eV, a tremendous theoretical breakdown electric field of 8 MV/cm, and a high Baliga's figure of merit, position it as a formidable contender for applications far exceeding the capabilities of Si, SiC, and GaN.[2,3] This has fueled remarkable progress in device research, with performance metrics for transistors and diodes advancing at an accelerated pace in recent years.[4–7]

While these properties are advantageous for all device architectures, the anisotropic nature of the monoclinic crystal structure means that the choice of crystal orientation is a critical design parameter for optimizing device performance. Theoretical calculations and experimental evidence have shown that electron mobility is highest along the crystallographic direction, which lies within the (010) plane. This makes the (010) surface a promising platform for fabricating high-performance lateral devices. In contrast, the (100) plane, while also explored, suffers from a natural cleavage tendency that complicates device processing and compromises mechanical stability. Despite the clear advantages of the (010) orientation, its development has been fundamentally hampered by the unavailability of large-area (010)-oriented substrates. Research has been consequently confined to small, often irregularly shaped samples cleaved from bulk crystals, which is unsuitable for scalable device fabrication and prohibits a meaningful assessment of wafer-scale uniformity.

The growth of high-quality, large-area single-crystal β-Ga_2O_3 is a foundational technology for advancing its electronic and optoelectronic applications. This is achieved through various melt-growth techniques, including the Czochralski (CZ),[8–10] edge-defined film-fed growth (EFG),[11–13] vertical Bridgman (VB),[14] and casting methods.[15,16] The ability to produce cost-effective native substrates from a melt gives Ga_2O_3 a significant advantage over other wide-bandgap semiconductors like SiC and GaN. The recent breakthrough in large-diameter crystal growth technology has led to the commercial availability of 2-inch diam-

†Corresponding author. E-mail: zhangsong02@163.com
‡Corresponding author. E-mail: xugw@ustc.edu.cn

© 2026 Chinese Physical Society and IOP Publishing Ltd. All rights, including for text and data mining, AI training, and similar technologies, are reserved.

eter (010) β-Ga_2O_3 wafers. This development creates an opportunity to transition (010) Ga_2O_3 from a subject of academic curiosity to a viable industrial technology. To capitalize on this advancement, the immediate and most critical task is to establish and validate a scalable, high-quality epitaxial growth process on this large-area platform.

Several epitaxial growth techniques have been explored, each with its own set of advantages and limitations. For instance, molecular beam epitaxy (MBE) offers unparalleled control at the atomic level but is often limited by slow growth rates,[17–20] while halide vapor phase epitaxy (HVPE) provides exceptionally high growth rates suitable for thick drift layers but can pose challenges for complex heterostructures and doping uniformity.[21–25] Metal–organic chemical vapor deposition (MOCVD) stands out as the premier technique for this purpose, given its proven success in the high-volume manufacturing of other compound semiconductors and its inherent advantages in controlling thickness, doping, and interface quality with high precision.[26–32]

In this paper, we report the first successful demonstration of homoepitaxial growth on a 2-inch, Fe-doped semi-insulating (010) β-Ga_2O_3 substrate via MOCVD. We present the first systematic, wafer-scale investigation of the material's properties, providing a comprehensive baseline for its structural perfection, surface morphology, and electrical uniformity. By demonstrating that device-quality films can be grown with high uniformity over a large area, our work validates the 2-inch (010) Ga_2O_3 platform and lays the essential groundwork for the future fabrication and commercialization of advanced lateral power electronic devices.

2. Experiment

The homoepitaxial films were grown in a horizontal flow MOCVD reactor on a 2-inch diameter, (010)-oriented β-Ga_2O_3 semi-insulating substrate with Fe doping. Prior to loading, the substrate was subjected to a standard solvent cleaning procedure. The growth was performed at a reactor pressure of 70 Torr and a substrate temperature of 830 °C. Triethylgallium (TEGa) served as the gallium precursor, high-purity molecular oxygen was the oxidant, and dilute silane (SiH_4) was the n-type dopant source. The V/III ratio was maintained at approximately 2000 during growth. These conditions resulted in a growth rate of about 0.6 μm/h. The epitaxial design, shown in Fig. 1(a), comprised a 20 nm $(Al_xGa_{1-x})_2O_3$ back-barrier layer with Al fraction of ∼ 20%, grown to suppress parasitic conduction at the epi-substrate interface, followed by a 200 nm thick Si-doped Ga_2O_3 channel layer targeted for a carrier concentration in the 10^{18} cm^{-3} range. To rigorously assess the film's uniformity, a comprehensive 9-point mapping pattern was established across the wafer, covering the center, middle, and edge regions, as illustrated in Fig. 1(b). Post-growth characterization involved a suite of non-destructive techniques: atomic force microscopy (AFM) to evaluate surface morphology, high-resolution x-ray diffraction (HRXRD) for crystalline quality and strain analysis, and mercury-probe capacitance–voltage (Hg-CV) measurements to determine the carrier concentration profile and its spatial distribution.

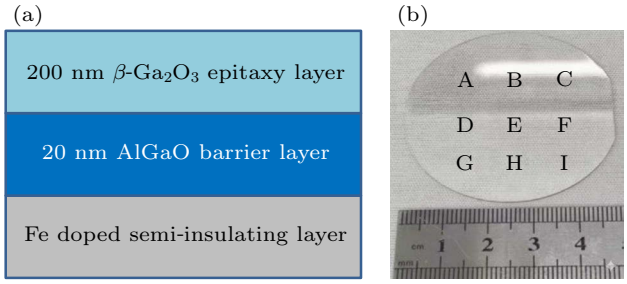


Fig. 1. (a) Schematic diagram of the MOCVD-grown epitaxial structure, consisting of a 200 nm Si-doped Ga_2O_3 channel layer and a 20 nm AlGaO back-barrier on an Fe-doped semi-insulating (010) β-Ga_2O_3 substrate. (b) Optical image of the 2-inch wafer illustrating the 9-point mapping locations (A through I) used for systematic characterization.

3. Results and discussion

The surface morphology of an epitaxial layer is a direct reflection of the growth kinetics and is paramount for device fabrication, as it dictates the quality of subsequent metallization and dielectric interfaces. Figure 2 displays the 5×5 μm^2 AFM scans from the nine designated points on the wafer. A striking feature across the entire wafer is the exceptionally smooth and well-ordered surface. Every measured location, from the center to the extreme edge, exhibits a distinct step-flow growth morphology. This morphology, characterized by long, parallel, and uniformly spaced atomic terraces, confirms

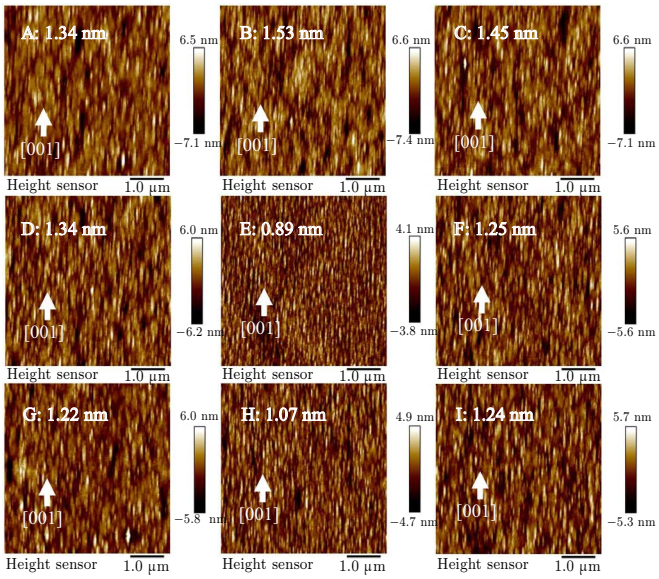


Fig. 2. Surface morphology and summary of structural properties. The 5 μm×5 μm AFM surface morphology scans for the nine designated points (A–I) across the 2-inch wafer all reveal a distinct step-flow growth mode, indicating an atomically smooth surface.

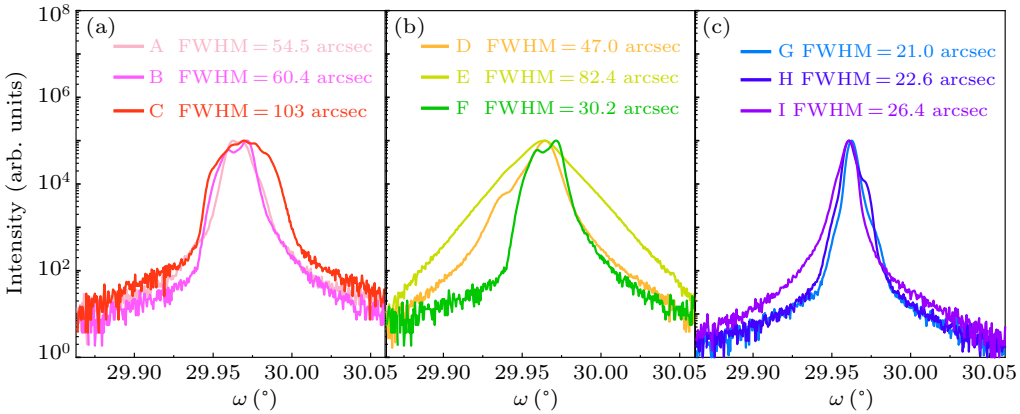


Fig. 3. High-resolution x-ray diffraction rocking curves for the symmetric (020) reflection.

that the growth proceeded in an ideal two-dimensional layer-by-layer fashion. This is achieved when the diffusion length of adatoms on the surface is sufficiently long for them to reach and incorporate at the step edges, a condition met by our optimized MOCVD process. The root-mean-square (RMS) roughness is low across the entire 2-inch area, with values tabulated in Fig. 2. The central region of the wafer (point E) shows the lowest RMS roughness of 0.89 nm, while the values remain below 1.53 nm at the wafer's edge. The relative standard deviation (RSD) is calculated to be 14.5%.

While some spatial variations are inherent to a new large-area process, the overall uniformity of the epitaxial film represents a significant advancement for the β-Ga_2O_3 material system. The crystalline quality and its uniformity were quantitatively assessed using HRXRD ω-rocking curve measurements of the symmetric (020) reflection. The full-width at half-maximum (FWHM) of the rocking curve is a sensitive measure of the crystalline perfection. The film demonstrates an outstanding crystalline structure, with FWHM values as narrow as 21.0 arcsec and 22.6 arcsec at points G and H, respectively. This result is significant as it proves that the MOCVD process can be readily adapted to the (010) surface to yield films of the highest structural quality. Interestingly, some peaks within this region, such as that from point F (FWHM $\approx$ 30.2 arcsec), exhibit a highly narrow main peak but with a subtle low-angle shoulder. The RSD of FWHM is calculated to be 54.2%. This asymmetric lineshape is often indicative of localized crystal imperfections. While it could suggest the presence of slightly misoriented crystalline domains or low-angle grain boundaries, other physical mechanisms such as localized strain gradients or a high density of specific types of dislocations cannot be ruled out. These features are likely inherited from the substrate or formed during the initial stages of growth.

The observed spatial variation in FWHM values ranges from 21.0 arcsec to 103.0 arcsec. This non-uniformity could originate from several factors. Firstly, variations in the crystalline quality of the starting 2-inch β-Ga_2O_3 substrate itself can be directly inherited by the epitaxial layer. Secondly, thermal gradients or non-uniform precursor flow dynamics across the large-area susceptor within the MOCVD reactor can lead to spatial differences in growth kinetics, thereby affecting crystalline perfection. Further optimization of both the substrate manufacturing and the MOCVD growth process is necessary to improve this wafer-scale uniformity.

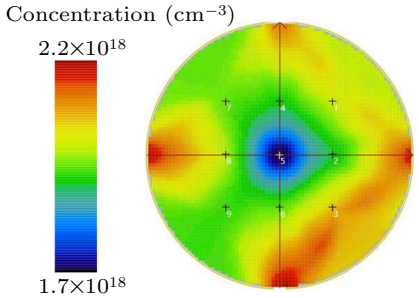


Fig. 4. Wafer-scale carrier concentration mapping. Spatial distribution map of the average carrier concentration across the 2-inch wafer, as determined by mercury-probe capacitance–voltage (Hg-CV) measurements. The color scale indicates the concentration in cm^{-3}. The map demonstrates good doping uniformity, with a slight center-to-edge variation.

For electronic device applications, precise control over the carrier concentration and its uniformity is non-negotiable. We employed Hg-CV profiling to map the electrical properties of the Si-doped channel. Figure 4 displays a color map of the average carrier concentration across the wafer. The map reveals a highly uniform doping profile, with an average concentration of 1.95×10^{18} cm^{-3} (RSD $\approx$ 5.12%). This uniformity is excellent for a nascent 2-inch process and is suitable for establishing consistent device threshold voltages during manufacturing. The spatial distribution shows a radial pattern, with the concentration being lowest at the center (1.71×10^{18} cm^{-3} at point E) and gradually increasing towards the edges. This trend is often attributed to the interplay between mass-transport-limited and kinetically-limited growth regimes,[33] which can affect the incorporation efficiency of dopant atoms like silicon. The depth profiles of the carrier concentration, plotted in Fig. 5 for all nine locations, provide further insight. The profiles are flat throughout

the channel, indicating that the silicon precursor flow was stable and its incorporation rate was constant during the entire growth run. This vertical uniformity is crucial for ensuring that the device characteristics do not vary with channel depth.

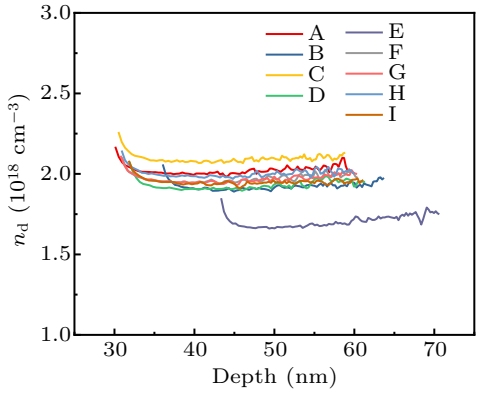


Fig. 5. Carrier concentration depth profiles. Carrier concentration (n_d) as a function of depth from the surface, measured by Hg-CV at the nine locations across the wafer. The profiles are flat and stable throughout the bulk of the 200 nm Ga_2O_3 channel layer, indicating uniform silicon incorporation during MOCVD growth.

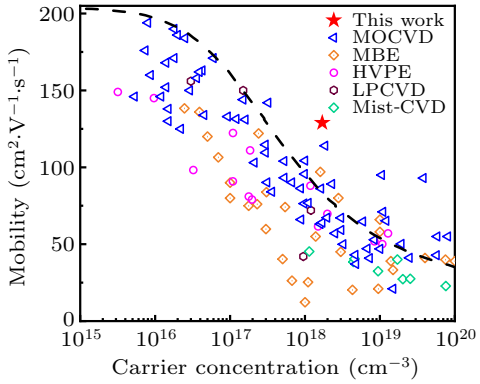


Fig. 6. Room-temperature Hall mobility benchmark. Electron mobility as a function of carrier concentration for the MOCVD-grown film on (010) β-Ga_2O_3 (red stars), compared with a compilation of literature data for β-Ga_2O_3 films grown on various orientations. The results from this work are positioned in the upper range of reported values, confirming the high electronic quality of the material.

To directly evaluate the electron transport properties, which are the primary motivation for using the (010) orientation, room-temperature Hall effect measurements were conducted. A sample from the center of the wafer yielded an electron mobility of 129 cm^2·V^{-1}·s^{-1}. At this relatively high doping concentration, electron mobility is primarily limited by ionized impurity scattering. The achievement of such a high mobility value is therefore a strong indicator of low background impurity levels and a low degree of compensation. When benchmarked against literature data for β-Ga_2O_3, as shown in Fig. 6, our result is positioned among the highest reported mobilities for this doping regime. It experimentally confirms that the theoretical potential of the (010) orientation can be realized in practice using a scalable MOCVD process on 2-inch wafers.

4. Conclusion and perspectives

In summary, we have successfully performed the first MOCVD homoepitaxial growth on a 2-inch (010)-oriented β-Ga_2O_3 substrate and conducted the first comprehensive, wafer-scale characterization of the resulting film. Our detailed investigation revealed outstanding material quality across the entire wafer, including an atomically smooth surface with a uniform step-flow morphology (with RMS roughness values between 0.89 nm and 1.53 nm), a superior crystalline structure with XRD rocking curve FWHM ranging from 21.0 arcsec to 103 arcsec. Furthermore, we demonstrated precise and uniform control over n-type doping, achieving a carrier concentration of $\sim 2 \times 10^{18}$ cm^{-3} with excellent spatial (RSD $\approx 5.12\%$) and depth uniformity. This pioneering demonstration not only establishes a robust baseline for device-quality material on a previously unavailable platform but also validates the manufacturability of the (010) β-Ga_2O_3 material system. This work represents a decisive step in advancing lateral Ga_2O_3 power devices from laboratory-scale concepts to a tangible, wafer-level technology poised for commercial impact.

Acknowledgements

This work was supported by the National Natural Science Foundation of China (Grant Nos. U23A20358, 62474170, 61925110, 62404214, and 62234007), the University of Science and Technology of China (USTC) Research Funds of the Double First-Class Initiative (Grant No. WK2100000055), the Project of the 46th Research Institute of CETC (Grant No. WDZC202446007), the JieBang Headed Project of Changsha City Hunan Province (Grant No. kq2301006), and the Opening Project and the Key Laboratory of Nano devices and Applications in Suzhou Institute of Nano-Tech and Nano-Bionics of CAS. This work was partially carried out at the Center for Micro and Nanoscale Research of USTC. The authors would like to thank Hangzhou Garen Semiconductor Company for providing the casting β-Ga_2O_3 bulk crystal and MicroAhead from Suzhou for CV test.

References

[1] Higashiwaki M, Sasaki K, Kuramata A, Masui T and Yamakoshi S 2012 *Appl. Phys. Lett.* **100** 013504
[2] Ma N, Tanen N, Verma A, Guo Z, Luo T, Xing H and Jena D 2016 *Appl. Phys. Lett.* **109** 212101
[3] Baldini M, Galazka Z and Wagner G 2018 *Mat. Sci. Semicon. Proc.* **78** 132
[4] Green A, Chabak K, Heller E, Fitch R, Baldini M, Fiedler A, Irmscher K, Wagner G, Galazka Z, Tetlak S, Crespo A, Leedy K and Jessen G 2016 *IEEE Electron Device Lett.* **37** 902
[5] Konishi K, Goto K, Murakami H, Kumagai Y, Kuramata A, Yamakoshi S and Higashiwaki M 2017 *Appl. Phys. Lett.* **110** 103506
[6] Zhou X, Ma Y, Xu G, Liu Q, Liu J, He Q, Zhao X and Long S 2022 *Appl. Phys. Lett.* **121** 223501
[7] Zhang J, Dong P, Dang K, Zhang Y, Yan Q, Xiang H, Su J, Liu Z, Si M, Gao J, Kong M, Zhou H and Hao Y 2022 *Nat. Commun.* **13** 3900
[8] Tomm Y, Reiche P, Klimm D and Fukuda T 2000 *J. Cryst. Growth* **220** 510

[9] Galazka Z, Irmscher K, Uecker R, Bertram R, Pietsch M, Kwasniewski A, Naumann M, Schulz T, Schewski R, Klimm D and Bickermann M 2014 *J. Cryst. Growth* **404** 184

[10] Galazka Z, Uecker R, Klimm D, Irmscher K, Naumann M, Pietsch M, Kwasniewski A, Bertram R, Ganschow S and Bickermann M 2017 *ECS J. Solid State Sci. Technol.* **6** Q3007

[11] Kuramata A, Koshi K, Watanabe S, Yamaoka Y, Masui T and Yamakoshi S 2016 *Jpn. J. Appl. Phys.* **55** 1202

[12] Fu H, Chen H, Huang X, Baranowski I, Montes J, Yang T and Zhao Y 2018 *IEEE Trans. Electron Devices* **65** 3507

[13] Mu W X, Jia Z T, Yin Y R, Hu Q Q, Li Y, Wu B Y, Zhang J and Tao X T 2017 *J. Alloys Compd.* **714** 453

[14] Hoshikawa K, Kobayashi T and Ohba E 2020 *J. Cryst. Growth* **546** 125778

[15] Xia N, Liu Y, Wu D, Li L, Ma K, Wang J, Zhang H and Yang D 2023 *J. Alloys Compd.* **935** 168036

[16] Yan Y, Wu D, Xia N, Deng T, Zhang H and Yang D 2024 *Appl. Phys. Lett.* **124** 122102

[17] Mauze A, Zhang Y, Itoh T, Ahmadi E and Speck J S 2020 *Appl. Phys. Lett.* **117** 222102

[18] Sasaki K, Higashiwaki M, Kuramata A, Masui T and Yamakoshi S 2013 *J. Cryst. Growth* **378** 591

[19] Liu X Z, Yue C, Xia C T and Zhang W L 2016 *Chin. Phys. B* **25** 017201

[20] Nepal N, Scott Katzer D and Meyer D J 2019 *Gallium Oxide* pp. 31–46

[21] Murakami H, Nomura K, Goto K, Sasaki K, Kawara K, Thieu Q T, Togashi R, Kumagai Y, Higashiwaki M, Kuramata A, Yamakoshi S, Monemar B and Koukitu A 2015 *Appl. Phys. Exp.* **8** 015503

[22] Higashiwaki M, Sasaki K, Goto K, Nomura K, Thieu Q T, Togashi R, Murakami H, Kumagai Y, Monemar B, Koukitu A, Kuramata A and Yamakoshi S 2015 2015 73*rd Annual Device Research Conference (DRC)*, pp. 29–30

[23] Higashiwaki M, Konishi K, Sasaki K, Goto K, Nomura K, Thieu Q T, Togashi R, Murakami H, Kumagai Y, Monemar B, Koukitu A, Kuramata A and Yamakoshi S 2016 *Appl. Phys. Lett.* **108** 133503

[24] Goto K, Konishi K, Murakami H, Kumagai Y, Monemar B, Higashiwaki M, Kuramata A and Yamakoshi S 2018 *Thin Solid Films* **666** 182

[25] Tadjer M J, Koehler A D, Freitas J A, Gallagher J C, Specht M C, Glaser E R, Hobart K D, Anderson T J, Kub F J, Thieu Q T, Sasaki K, Wakimoto D, Goto K, Watanabe S and Kuramata A 2018 *Appl. Phys. Lett.* **113** 192102

[26] Hellwig M, Xu K, Barreca D, Gasparotto A, Niermann B, Winter J, Becker H W, Rogalla D, Fischer R A and Devi A 2009 *Ecs Transactions* **25** 617

[27] Du X, Mi W, Luan C, Li Z, Xia C and Ma J 2014 *J. Cryst. Growth* **404** 75

[28] Gogova D, Wagner G, Baldini M, Schmidbauer M, Irmscher K, Schewski R, Galazka Z, Albrecht M and Fornari R 2014 *J. Cryst. Growth* **401** 665

[29] Wagner G, Baldini M, Gogova D, Schmidbauer M, Schewski R, Albrecht M, Galazka Z, Klimm D and Fornari R 2014 *Phys. status solidi (A)* **211** 27

[30] Du X, Li Z, Luan C, Wang W, Wang M, Feng X, Xiao H and Ma J 2015 *J. Mater. Sci.* **50** 3252

[31] Alema F, Zhang Y W, Osinsky A, Valente N, Mauze A, Itoh T and Speck J S 2019 *APL Mater.* **7** 121110

[32] Feng Z X, Bhuiyan A F M A U, Karim M R and Zhao H P 2019 *Appl. Phys. Lett.* **114** 250601

[33] Theodoropoulos C, Ingle N K, Mountziaris T J, Chen Z Y, Liu P L, Kioseoglou G and Petrou A 1995 *J. Electrochem. Soc.* **142** 2086